Materials Today Communications 6 (2016) 50–55

Contents lists available at ScienceDirect

Materials Today Communications

journal homepage: www.elsevier.com/locate/mtcomm

Fabrication and characterization of polymer membranes with integrated arrays of high performance micro-magnets

Damien Le Roy[a,b,*,1], Gorky Shaw[a,b], Richard Haettel[a,b], Klaus Hasselbach[a,b], Frédéric Dumas-Bouchiat[a,b,c], Dominique Givord[a,b], Nora M. Dempsey[a,b]

[a] Univ Grenoble Alpes, Inst NEEL, F-38042 Grenoble, France
[b] CNRS, Inst NEEL, F-38042 Grenoble, France
[c] Univ Limoges, CNRS, ENSCI, SPCTS, UMR 7315, F-87000 Limoges, France

ARTICLE INFO

Article history:
Received 4 September 2015
Received in revised form
16 December 2015
Accepted 23 December 2015
Available online 29 December 2015

Keywords:
Magnetic membranes
Micro-magnets
Bio-MEMS

ABSTRACT

Micro-fabrication techniques (lithography, deep reactive ion etching and sputtering) have been used to prepare regular arrays of micro-magnets on the surface of topographically patterned Si substrates. These arrays, composed of either high magnetization soft magnetic $Fe_{65}Co_{35}$ or high coercivity hard magnetic Nd–Fe–B, were embedded in a polymer matrix of polydimethylsiloxane which could be mechanically peeled off the Si substrate to produce free standing magnetic membranes. Scanning Hall probe microscopy was used to measure the stray field patterns produced at distances in the range of 10–50 μm above the membranes. The level of control achieved over the shape, size and spatial distribution of the hard or soft magnetic elements, combined with the transparency, flexibility and biocompatibility of the polymer matrix, renders the composite membranes attractive for use in micro-systems in general and bio-micro-systems in particular.

1. Introduction

Contactless actuation in microsystems has attracted much attention in the past decades. Compared to approaches based on acoustics [1], hydrodynamics [2], optics [3], or dielectrophoresis [4], magnetism offers a unique combination of large, bidirectional forces without the requirement for on-chip power. A widely explored example is the development of magnetically responsive membranes for use in micro-pumps [5–9], in which an external magnetic field source controls the membrane deflection. Another promising application is the development of air separation devices that exploit the molecules intrinsic magnetic susceptibility [10]. In emerging biotechnologies, magnetism has proved to be an efficient means for the remote control of nanoparticles, to serve various functions including cell manipulation [11,12], trapping of drug vectors [13], or the application of highly local mechanical strain in living organisms [14,15]. The associated volume force, known as the magnetophoretic force, is given by: $\boldsymbol{F} = (\boldsymbol{M} \cdot \nabla)\boldsymbol{B}$, where M is the magnetization vector of the object, and B the induction vector of the magnetic field source. Micrometer sized magnets can produce magnetic field gradients of up to 10^6 T/m, though the range of significant magnetic interaction drops quickly with distance, typically being limited to some tens of micrometers. Micro-magnet arrays have been produced by various techniques, from film patterning to powder positioning. Magnetic films have been patterned by depositing them on patterned resin masks and then performing lift-off [16,17], depositing them onto topographically patterned Si substrates and chemical etching of the magnetic film [18], or using local magnetization switching in magnetically-hard films [19]. The controlled positioning of magnetic powders has been obtained by soft lithography of matrix-embedded powder [20], dry-pressing of powder into pre-etched substrates [21] or using magnetic moulds [22,23]. Film-based approaches give the greatest control over the magnetic pattern (size, shape and position of individual features) though the application of film-based structures may be limited by both the mechanical and optical properties of the substrate used. Powder-based approaches are typically low cost, easy to implement and have the advantage that the properties of the matrix may be tuned to suit the application.

In this paper we report on the fabrication of polymer membranes containing regular arrays of micro-magnets. The approach combines the advantages of having control over the magnetic properties afforded by film patterning and control over the mechanical and optical properties provided by the polymer matrix. Structures based on both hard and soft micro-magnet arrays have been

* Corresponding author.
E-mail address: damien.le-roy@univ-lyon1.fr (D.L. Roy).
[1] This author is now at the Institut Lumière Matière, Université Lyon 1-CNRS, Villeurbanne, France.

http://dx.doi.org/10.1016/j.mtcomm.2015.12.004
2352-4928/

produced. Once magnetized, hard magnet based structures have a fixed stray field pattern, thus they produce a fixed force on a given target object at a given position. On the other hand, the stray field pattern produced by soft micro-magnets can be easily modulated by simply varying the value of the magnetic field applied to magnetize them, so that the force produced on a target object can be easily varied. After describing the process itself, we will show how parameters influence the depth of the micro-magnets below the membrane surface, and thus the effective working distance, and the surface planarity. We will present the magnetizing characteristics of soft-magnet arrays and then measurements of the magnetic stray field patterns produced above soft and hard micro-magnet based structures. Finally we will discuss the relative pros and cons of using soft or hard micro-magnet arrays.

2. Fabrication process

The process used to fabricate the composite membranes, hereafter referred to as magnetic membranes, is schematized in Fig. 1. Arrays of micrometer-size Si pillars are produced at the surface of a Si substrate using deep reactive ion etching (DRIE) through a sputtered 200 nm-thick Al mask obtained by lift-off, following the time-multiplexed plasma etching recipe originally introduced by Laemer and Schilp [24] and commonly referred as the Bosch process. Under standard conditions, the Bosch process permits one to achieve vertical structures. However, to reduce the tearing resistance of the pillars, in view of transferring them into the polymer membrane, it is possible to slightly over etch, as schematized in Fig. 1, by increasing the time of the plasma etching phases with respect to the passivation phases. In this report, we

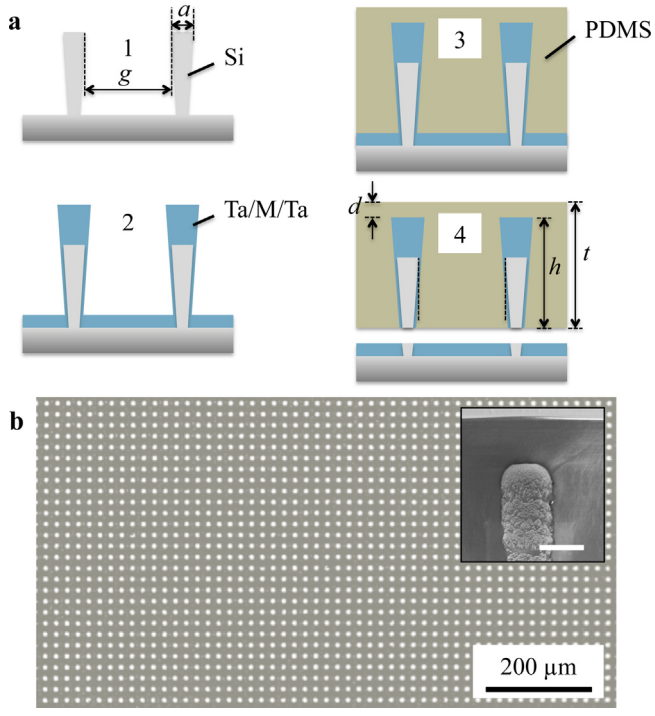

Fig. 1. (a) Schematic diagram of the fabrication process. (1) Deep reactive ion etching of a Si substrate. (2) Deposition of a Ta/*M*/Ta trilayer (*M* = Fe–Co or Nd–Fe–B), by high rate sputtering onto the patterned Si substrate. (3) Application of liquid PDMS over the magnetic pillar array and reticulation. (4) Peeling-off mechanically of the magnetic membrane. (b) Plan view image of a free standing magnetic membrane (optical microscope) containing 10 μm wide magnetic pillars. The inset shows a side view of the top of a magnetic pillar embedded in the PDMS membrane. The scale bar in the inset represents 10 μm.

focus on pillars of 10 μm and 25 μm width and fixed height of 45 μm, with the same over-etch angle of 8°.

The topographically patterned Si substrates are then covered with Ta (100 nm)/*M* (10 μm)/Ta (100 nm), with *M* = Fe–Co or Nd–Fe–B, using high-rate triode sputtering [25], from alloy target with compositions of $Fe_{65}Co_{35}$ and $Nd_{14}Fe_{80}B_6$, respectively. The Ta buffer layer serves to prevent the magnetic layer from alloying with the Si substrate while the capping layer protects it from oxidation. The total height of the transferred pillar will hereafter be denoted *h* (see Fig. 1). Note that no power was supplied to the substrate heater during deposition. The as-grown $Fe_{65}Co_{35}$ films are crystallized in a *bcc* structure, and show [110] fiber-textured (X-ray diffraction and pole figure data not shown). The amorphous as-grown Nd-Fe-B films are *ex situ* annealed at 550 °C for 10 min to crystallize randomly oriented grains of the magnetically hard $Nd_2Fe_{14}B$ phase (X-ray data not shown).

PDMS is prepared by mixing 10/1 w/w of monomer and curing agent, respectively (Sylgard from Samaro). The mixture is thoroughly stirred and subsequently degased under vacuum. The liquid PDMS is then poured over the magnetic pillar array and spread by spinning for 30 s at rotation speeds of 1000–4000 rpm, resulting in a membrane thickness (*l*) ranging from 40 to 200 μm. A precise control of *l* enables us to control the distance from the upper surface of the membrane to the individual micro-magnets topping each pillar, hereafter-denoted *d*. The value of *l* was measured by Scanning Electron Microscopy (SEM) observations of sample cross-sections, with an estimated error of less than 2%. The dependence of *l* on the rotation speed *s*, for square pillar arrays with varying inter-pillar gap (*g*), are shown in Fig. 2(a). Test samples had a fixed surface area of 1 cm^2 in order to keep similar edge effects during spin coating.

After curing at 100 °C for 1 h, the PDMS forms a solid membrane encapsulating the micro-pillars. For the slowest rotation speed *s* of 1000 rpm, the membrane thickness *l* is found to be close to 200 μm, independent of the inter-pillar gap *g*. When *s* increases, *l* decreases and approaches the total pillar height *h*. For *s* of 2000 rpm and above, the dependence of *l* on *g* is clearly observed, following the general trend that *l* decreases as *g* increases. For sparse arrays (i.e., large inter-pillar gap) and high values of *s*, the membrane can be thinner than the height of the embedded pillars ($l/h \leq 1$). For samples with *l*/*h* greater than 1 (see the inset of Fig. 1(b)), the distance from the surface of the membrane to the top of the micro-magnets, *d*, is simply given by $d = l - h$. Atomic force microscopy was used to measure the roughness of the surface of the membrane, as characterized by the peak-to-peak values of the surface modulation, Δd, as a function of *d* (Fig. 2(b)). The modulation reveals the periodic pattern of the underlying pillar array. For a pillar width and inter-pillar gap of 10 μm and for $d \geq 12$ μm, the peak-to-peak modulation is less than 100 nm, as extrapolated from Fig. 2(b). The cured PDMS can be mechanically peeled off the underlying Si substrate to produce a free standing membrane containing embedded micro-magnets of well defined geometry. The transfer yield, determined from optical microscope observations, was found to depend on the pillar dimensions. The 10 μm pillars all transferred into the PDMS membrane, while around only 15% of 25 μm pillars were transferred, for the same degree of DRIE over etch. For similar pillar height, the tensile and shear stresses that are applied during peel-off scale as the inverse of the pillar's section, which explains why small-section pillars transfer more easily.

In the case of hard magnet based membranes, the final step in the fabrication process concerns magnetizing the micro-magnets in an external magnetic field. The Nd–Fe–B containing membranes reported here, which had a coercive field of 2 T, were magnetized along the long axis of the pillars, in a field of 6 T. A representative magnetization curve of such membranes, measured in the out-of-plane direction, is shown in Fig. 3(c). In the case of soft magnet based membranes, which have no remanent